

HDPE Liquefaction: Random Chain Scission Model

PRIYA RANGARAJAN, DIBAKAR BHATTACHARYYA, ERIC GRULKE

Department of Chemical and Materials Engineering, University of Kentucky, Lexington, Kentucky 40506-0046, USA

Received 6 October 1997; accepted 30 April 1998

ABSTRACT: Liquefaction of commodity polymers to oils and gases can be used to recover the energy value of these materials. This article reports liquefaction data for high-density polyethylene (HDPE), one of the major plastics in recycled material. Thermal degradation of HDPE to oil-gas mixtures required higher temperatures (450–490°C) than low-density polyethylene (LDPE) (430–460°C) because of fewer chain branching points for HDPE, which are more susceptible to chain scission reactions. The addition of hydrogen (0.1–1.5 MPa) had negligible effect on product distribution. HDPE thermal degradation is consistent with a random chain scission mechanism. Product distributions for degradation at 450°C were modeled assuming random chain scission with a rate constant $k(x)$ dependent on the molecular weight x by a power law model dependence, $k(x) = k_b x^b$, where k_b is the pseudo-first-order rate constant, and b is the power index of dependence on molecular weight. Degradation rates dropped rapidly after initial breakup of the chains, and 2 sets of coefficients were needed to describe the molecular weight distributions as functions of reaction time. The error in model was about 10%. This model can be used to optimize the production of oils from thermal degradation of HDPE. © 1998 John Wiley & Sons, Inc. *J Appl Polym Sci* 70: 1239–1251, 1998

Key words: high-density polyethylene; chain scission; liquefaction; log-normal molecular weight distribution; kinetics

INTRODUCTION

Polymer Liquefaction

Dumping of industrial and post-consumer waste is proving to be a costly waste disposal option.^{1,2} Plastics are versatile in their recyclable options, which may include reuse as solids, recycling as monomer, and recycling as energy (via combustion, gaseous fuel feedstocks, or liquid fuel feedstocks). Polymer gasification has been well studied, but little attention has been paid to producing oligomer and liquid fuels. Cracking polymers to hydrocarbon feedstocks for existing petrochemical processes recovery is a viable solution for retrieving the fuel value of plastics. Liquefaction

refers to the thermal or catalytic breakdown of large chain molecules to form liquid fuels. Coal liquefaction is usually done in the presence of hydrogen to increase the H : C ratio and hence improve the fuel value of the liquid. Production of liquid fuels from polymers may not require the addition of hydrogen since these materials have high H : C ratios.

Thermal and catalytic degradation studies of a variety of polymers have been conducted under pyrolysis conditions,^{2,3} in solution,^{4,5} and with^{2,3,6} or without catalysts,^{1,3,7–10} and solvents.^{1,3,5,10} Most commodity polymers undergo chain scission to form a range of polymer, oligomer, and monomer products. Degradation to monomer would be convenient, yet only a few polymers yield high levels of their original monomers.

Liquid degradation processes can be interpreted kinetically using moments from their molecular weight distributions (MWDs). Kinetic

Correspondence to: E. A. Grulke (phone: (606) 257-4958; fax: (606) 323-1929; email: egrulke@engr.uky.edu).

Journal of Applied Polymer Science, Vol. 70, 1239–1251 (1998)

© 1998 John Wiley & Sons, Inc.

CCC 0021-8995/98/061239-13

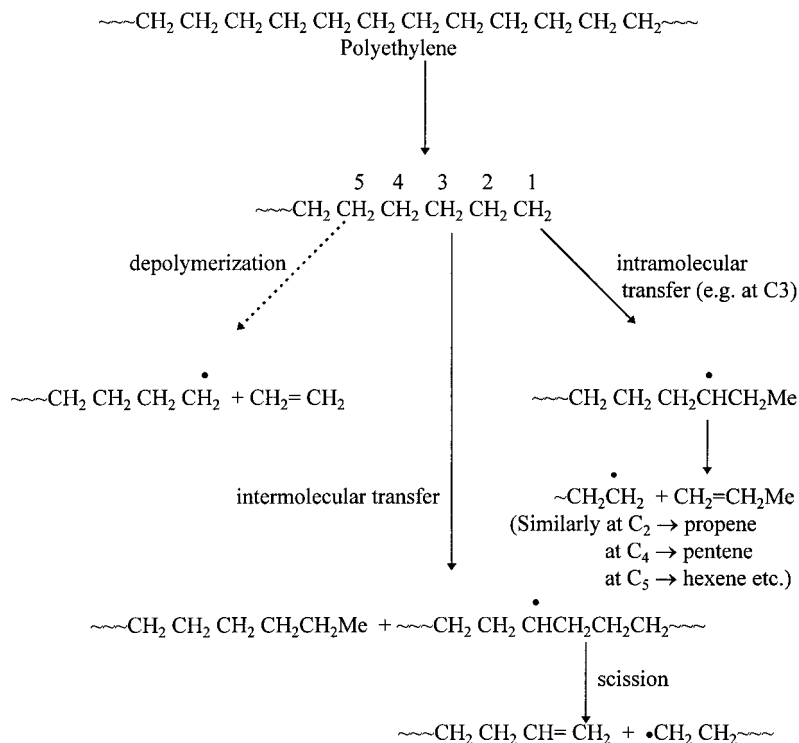


Figure 1 Various mechanistic pathways for degradation of polyethylene.¹⁴

models of continuous mixtures have been applied to a variety of degradations, such as poly(methyl methacrylate),⁵ poly(styrene allyl alcohol),^{4,11} and coal.^{12,13} These models assume that chain scission does not depend on chain length and may include terms for specific products that form as part of the mechanism.

This work studied the production of oligomers and liquids from an important recyclable polymer, HDPE. It has a high H : C ratio (2 : 1) and a relatively simple structure, and it is a major component in many plastic waste streams. Data on LDPE degradation¹ and preliminary data on HDPE degradation suggested that both polyethylenes quickly break down to shorter chains, which then degrade at lower rates. There are 2 simple ways to analyze this performance. The degradation could be modeled by the following 2 mechanisms: branch point scission and random chain scission. This would require analysis of the branch site fraction in the polymer and 2 sets of kinetic parameters. An alternative method is to use chain-length-dependent kinetics. The integrodifferential equations would then be solved using a noninteger power for the chain length dependence. The kinetic parameters would be specific to a given HDPE sample.

The objective of this research was to measure product distributions from the liquefaction of HDPE (with and without hydrogen in the reactor) and model these using chain-length-dependent degradation kinetics. This type of model can be used to optimize the product distribution from polymer liquefactions.

Development of a Chain-Length-Dependent Chain Scission Model

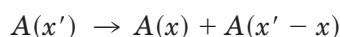
Mechanism

Figure 1 summarizes the thermal degradation mechanism for linear polyethylene.¹⁴ Chain scission degradation can be sensitive to temperature, pressure, concentrations, and solvents. There are 3 major processes, as follows: depolymerization of the chain end to monomer, intramolecular transfer at a chain end to produce light fractions, and intermolecular transfer resulting in random chain scission to produce shorter chain segments. When branching sites are present, they also dissociate to form chain fragments. Branch sites are known to be more unstable than linear chains. A complete model would include separate rate constants for each linear chain process plus rate constants for the branch sites. We have ignored de-

polymerization to monomer and intramolecular transfer producing short chains and have lumped all the mechanisms into a general chain scission model; this is justified by data showing the short fragments are not major products of polyethylene degradation. Depolymerization to ethylene constitutes only 3% of the product distribution,¹⁵ and unsaturated gaseous products tend to be less than 10% of the product distribution. Researchers working with model compounds¹⁶ (C₉ to C₂₂) have shown that chain scission rates depend on the chain length. Therefore, we expected that long chains should also exhibit chain-length-dependent degradation rates. This approach is suitable for describing the formation of liquid oligomers but may not apply if gaseous products are desired.

Modeling by Continuous Kinetics Approach

Continuous mixture kinetics describe the binary fragmentation of polymer particles.^{4,11,17} Binary fragmentation assumes that chains split into 2 pieces for any single event, resulting in a distribution of chain lengths. This is a reasonable assumption except in cases with extremely high degradation rates. A polymer molecule, $A(x')$, with an initial molecular weight of x' , breaks into 2 fragments, $A(x)$ and $A(x' - x)$, as follows:



If $k(x)$ is the degradation rate constant, the change of molecular weight, x , due to degradation is

$$\frac{dx}{dt} = x \cdot k(x) \quad (1)$$

During random degradation, the original distribution is shifted to one with lower molecular weights. If there is a model for the original MWD, then the product MWDs can be related to the parameters of the original distribution, the reaction time, and chain scission rate constants.^{4,11} Chain length dependence of the degradation rate can be introduced in equation (1) by letting $k(x)$ be a function of x , as follows:

$$k(x) = k_b(x)^b \quad (2)$$

where b is a real number. When $b = 0$, the chain scission mechanism is independent of the chain length.

The population balance for a single chain of molecular weight x is

$$\frac{\partial x}{\partial t} = 2 \int_x^\infty k(x')x\Omega(x, x') dx' - k(x)x \quad (3)$$

The second term on the RHS accounts for loss of reactant, $A(x)$, due to its degradation [eq. (1)], while the first term denotes the gain of $A(x)$ resulting from degradation of polymer molecules with molecular weights larger than x . The factor 2 accounts for the binary fragmentation process, that is, when a molecule breaks into 2 daughter molecules, there are 2 ways by which a molecule of certain molecular weight can result from a parent molecule. The stoichiometric kernel, $\Omega(x, x')$, is the fraction of $A(x')$ that cracks to $A(x)$.¹⁷ For a total random kernel, the products are equally distributed along all $x' \leq x$, and we obtain

$$\Omega(x, x') = \frac{1}{x'} \quad (4)$$

This implies that a molecule of size x' has a probability of $1/x'$ to divide into 2 molecules $x' - x$ and x . The initial MWD, $p_0(x)$, is

$$p(t = 0, x) = p_0(x) \quad (5)$$

Equations (3)–(5) have been solved using the moments method⁴ based on $p_0(x)$ being a Gaussian distribution. The degradation rate coefficients can be found using the first 3 moments of the reactant and product MWDs. Analytical solutions are available for b values of 0⁴ and 1.¹¹ A simplified numerical method provides solutions for integer values of $b > 1$.¹¹

Model Application to HDPE Liquefaction

The moments method can be applied to the degradation of HDPE, as follows. All degradation processes were modeled as chain scission, assuming an apparent first-order rate equation [eq. (1)]. We also assumed that the presence of hydrogen did not affect the degradation mechanism. Assessing the effects of hydrogen would require product separation by molecular weight and C=C content. The second analysis was not present in our laboratory. We have assumed that no crosslinking or repolymerization occurs. Model

compound studies have shown the existence of trace levels of such side reactions.¹⁸ We have not incorporated a specific step for scission at chain branch sites (tertiary carbons). This step would be based on measurement of tertiary carbons in the polymer, possibly by nuclear magnetic resonance (NMR) characterization. We are evaluating the simpler approach to determine whether it is adequate for engineering analyses of degradation processes.

EXPERIMENTAL

Materials

HDPE pellets of molecular weight 125,000 were purchased from Aldrich Chemical Company. Gel permeation chromatography (GPC) calibration standards were polyethylenes of low polydispersity, purchased from Scientific Polymer Products. A mixed plastic waste stream (Duales System Deutschland DSD Plastics) containing nearly 80% PE was used.

Liquefaction Experiments

The liquefaction experiments were conducted in a 50-mL microautoclave batch reactor. The reactor was initially charged with ~ 10.0 g of HDPE and could be pressurized with hydrogen. It was heated to a predetermined temperature in a fluidized sandbath agitated at 400 rpm. The runs were carried out typically for 30 min. At the end of the run, the reactor was air-cooled. The liquid products were analyzed by GPC (solids and waxes) and simulated distillation (liquids) techniques.

The preferred method (method 1) for operation was to drop the microreactor into the sandbath maintained at 480°C. The sandbath temperature set point was then lowered immediately to 450°C. Calculation and experience showed that overall system temperature approached 450°C in less than 5 min. The zero time for degradation was taken to be when 450°C was reached. Samples of polymer were taken from the microreactor at zero time in order to determine the actual initial molecular weight distribution for isothermal kinetic data.

An alternative operating method (method 2) equilibrated the reactor with the sandbath at 300°C and then changed the set point to 450°C. This required a much longer heat-up period and

gave lower initial molecular weights. As before, the zero time for isothermal kinetics was taken to be the instant when the sandbath reached 450°C.

Analyses

The thermogravimetric analysis (TGA) characterization of the original samples and the kinetic runs was done on a TGA 7 Perkin–Elmer instrument in order to study the heat history of degradation. The nitrogen flow rate was 40 mL/min, and the rate of heating was 10°C/min. MWDs were determined using a 150C Waters GPC with 4 high-temperature (HT) columns (140°C with 1,2,4-trichlorobenzene as the mobile phase). The injection volume was 200 μ L and the flowrate was 1 mL/min. The polymer concentration varied between 0.1 to 0.25 wt %. For lower MW calibration, (MW < 500), alkane samples were used. The GPC curves were digitized (response versus time) and converted to weight frequency versus molecular weight using the calibration curve. The liquid products were analyzed by simdistillation on a Perkin–Elmer Automated GC with FID detector.

Mixed Plastics

Mixed plastics were degraded in the microreactor over a range of temperatures (415, 420, 425, and 435°C) and for 2 reaction times, 30 and 60 min, using a previous operating method.¹ Remaining solids were extracted using tetrahydrofuran (THF) and pentane. GPC analysis was done on all fractions.

RESULTS AND DISCUSSION

This section is divided into 3 parts. Part 1 deals with the experimentally determined effect of liquefaction on the product distribution. Part 2 is the application of random chain scission to model liquefaction kinetics of HDPE. Part 3 reports the measurement and analysis of waste plastic mixture degradations.

Part 1: Effect of Liquefaction Parameters on Product MWDs

We have studied the effect of chain branching, temperature, and pressure on product distribution and yield.

Table I Effect of Temperature on Liquefaction Product Distribution Characteristics: 1.5 MPa Hydrogen (Initial) and 30-Min Reaction Time

Temperature (C)	< C ₆ (%)	C ₇ -C ₁₁ (%)	C ₁₂ -C ₁₅ (%)	> C ₁₅ (%)	Oil : Gas (%)
440	—	—	—	100	—
450	10.5	14.6	16.4	58.4	75 : 25
460	11.1	24.5	17.2	47.1	70 : 30
490	7.4	46.9	19.9	16.1	30 : 70

Effect of Chain Branching

The original HDPE sample had a number-average and weight-average molecular weight (M_n and M_w) corresponding to 97,600 and 186,000, respectively. At 440°C and 1.5 MPa hydrogen (cold), no liquid products were observed for a 30-min run. The solid residue remaining was subjected to GPC analyses and revealed a M_n and M_w equal to 1500 and 3870. The break down process yielded a lower molecular weight solid product. The liquefaction of LDPE¹ under identical conditions yielded 41% of oils + gases. We believe that this difference can be attributed to the chain branching differences between the two plastics. HDPE is a linear molecule containing about 3 branches/1000 carbon atoms, whereas LDPE has about 30 short and long chain branches/1000 carbon atoms. Thus, it is more probable that these branches could undergo chain scission in LDPE, yielding oil fractions faster. This can also be corroborated from the data of Uddin et al.,³ which showed that, under similar conditions, LDPE degraded to lower molecular weights at much high rates. Kossiakoff and Rice,¹⁹ and Voge and Good¹⁶ determined the stability of primary : secondary : tertiary carbon radicals. Extrapolating these stabilities to 450°C gives stability ratios of 1 : 16.1 : 261. Therefore,

tertiary carbons would be expected to have scission rates over an order of magnitude higher than those of secondary carbons.

Effect of Temperature

The HDPE sample was liquefied for 30 min at various temperatures and 1.5 MPa hydrogen (cold). The oil fraction is optimum between 450 and 460°C, with nearly complete conversion of the polymer into gaseous and liquid products. Table I shows the different fractions of oil produced. Liquefaction of polymers to maximize oil recovery should be carried out at lower temperatures (~ 450°C) or higher temperatures with short residence times. These conditions will decrease the rate of gas formation.

Effect of Pressure

Table II shows the effects of hydrogen pressure on liquefactions at 460 and 490°C. At both temperatures, the oil yield remained constant. However, there were modest changes in the gasoline, kerosene, and heavy oil fractions. At higher pressures, about 5% higher light fractions (C₇-C₁₁) and corresponding lower heavier fractions (>C₁₅) were formed. The difference in the product distributions, as analyzed by simdistillation, are within

Table II Effect of Initial Reactor Pressure on Liquefaction Product Distribution Characteristics (30-Min Reaction Time)

Pressure (MPa)	< C ₆ (%)	C ₇ -C ₁₁ (%)	C ₁₂ -C ₁₅ (%)	> C ₁₅ (%)	Oil : Gas (%)
460°C					70 : 30
0.8, H ₂	10.8	20.4	16.5	52.3	
1.5, H ₂	11.1	24.5	17.2	47.1	
490°C					30 : 70
1.5, H ₂	7.4	46.9	19.9	16.1	
1.5, N ₂	10.5	42.2	16.1	23.2	

the experimental error, and no significant effects of hydrogen pressure can be claimed. Other literature^{20,21} showed that hydrogen pressure suppressed the formation of heavier oil fractions. We also compared the effect of hydrogen and nitrogen pressures at 490°C and 1.5 MPa total pressure. The oil yield was found to be the same (~ 30%), but higher levels of lighter and middle fractions are formed with hydrogen as compared to nitrogen. When the polymer chain is cracked in the presence of hydrogen, capping of chain ends may occur. Other workers²⁰ reported better yield of lighter fractions under nitrogen at lower temperatures.

Hydrogen pressure did not significantly affect product distributions and may not be needed for HDPE degradation to liquid fuels, in contrast to coal liquefaction. This finding could reduce the expenses for recycling HDPE to liquids. The unsaturated liquid product might be fed directly to a refinery for hydrogenation and other treatment.

Part 2: Kinetics Analysis of Chain Scission Process

Log-Normal Distribution

McCoy and Wang¹¹ have chosen the gamma distribution function as a representative function for describing the molar and weight distributions of a variety of materials like coal liquid¹² and polymers.^{4,5} The log-normal distribution is preferred for many polymer systems, as follows:

$$p(x) = \frac{1}{\sqrt{2\pi}} \frac{1}{\sigma} \exp\left(-\frac{(\ln(x) - \ln(M_m))^2}{2\sigma^2}\right) \quad (6)$$

where M_m is the median value, and σ is the variance of the distribution. The variance, median value, and the various molecular weight averages are related by

$$\sigma = \sqrt{\ln\left(\frac{M_w}{M_n}\right)} \quad (7a)$$

$$M_m = M_n \exp\left(\frac{-\sigma^2}{2}\right) = M_w \exp\left(\frac{\sigma^2}{2}\right) \quad (7b)$$

where M_w and M_n are the number- and weight-average molecular weight of the MWD given as p^2/p^1 and p^1/p^0 , respectively, where p^2 , p^1 , and p^0 are the second, first, and zeroth moments of the MWD. Log-normal distribution functions gave the highest correlation coefficients (0.98 and

0.97 for reactants and products, respectively) for fitting our data. The mole-fraction distributions were computed from the GPC weight fraction distributions using

$$p_w(x) = p_n(x) \cdot x \quad (8)$$

Data Analysis by Numerical Moment Approach

The population balance kinetic model [eq. (3)] can be related to changes in the moment distributions as a function of time. For example, the zeroth, first, and second moments are related to k_b , b , and p by

$$\frac{dp^0}{dt} = k_b \cdot p^b \quad (9)$$

$$\frac{dp^1}{dt} = 0 \quad (10)$$

$$\frac{dp^2}{dt} = -\frac{1}{3} k_b \cdot p^{b+2} \quad (11)$$

The objective of the data analysis was to find the values of k_b and b that best fitted the time-dependent product distribution data. We computed the value of the dimensionless parameter $k_b \cdot t$, which is the product of the k_b and reaction time t . A higher value of $k_b \cdot t$ denotes greater degradation. Integer values of b did not give good predictions of the product distributions. Comparison of the data with analytical solutions demonstrated that b should range between 0 and 1. We developed a numerical procedure to solve equations (9)–(11) for noninteger values of b .

The 4th-order Runge–Kutta method was used to solve equations (9)–(11) by using initial guess values of k_b and b . The first moment p^1 is always unity since it is normalized. M_w and M_n are also related to the time derivatives of the moments. For every time interval, the zeroth and second moments were computed along with as the b th and the $b + 2$ th moments. These were used to improve the guesses for k_b and b since we know the new values of the zeroth and second moments. The numerical moments method for the log-normal distribution function was verified for $b = 0, 1, \text{ and } 2$ (Fig. 2; less than 3% error). The solutions for these coefficients are given in Appendix.

The parameters k_b and b have specific effects on product distributions. The value of k_b is a temperature-dependent multiplication constant

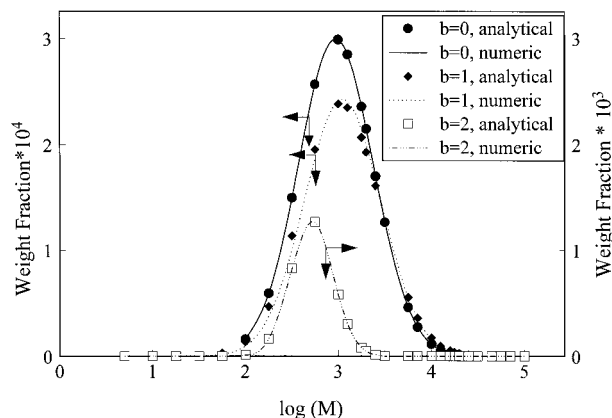


Figure 2 Log-normal molecular weight distribution curve for $b = 0, 1.0,$ and 2.0 : Comparison between analytical and numeric solutions.

and can be assumed to be the pseudo-first-order rate constant, whereas b is a index value for the moment derivatives with time. M_m is most sensitive to changes in k_b , whereas the distribution width σ is more dependent on b .

Our objective was to find a set of parameters that best describe the family of product distributions from a series of isothermal conditions. We first found parameters k_b and b for each individual distribution by relating it to the zero time distribution. The standard deviations of the product distributions were well behaved, and it was convenient to first select b and then find k_b . Values of b were tested over the range of 0.7 to 1.0.

For the method 2 runs, the best-fit values were $k_b = 1.5 \cdot 10^{-4} \text{ min}^{-1} (\text{g/gmol})^{-0.85}$ and $b = 0.85$. These parameter values predict the data well. Errors, computed as the square root of the summation of the squares of the relative errors of the experimental and model M_n and M_w , were less than 10%.

Figure 3 shows the values (calculated and experimental) of molecular weight distribution obtained from the log-normal distribution of the weight fraction MWDs of the 450°C runs (method 1). The product distributions shift to the left as degradation time increases. Figure 4 shows that the molecular weight averages M_n , M_w and M_m decrease as the degradation time increases. Experimental points are shown, and the model results are given as continuous curves. The zero time run for method 1 has a larger M_w and M_n than that found for method 2. This can be attributed to the shorter heat-up time for method 1 (5 min) as compared to method 2 (typically 1 h).

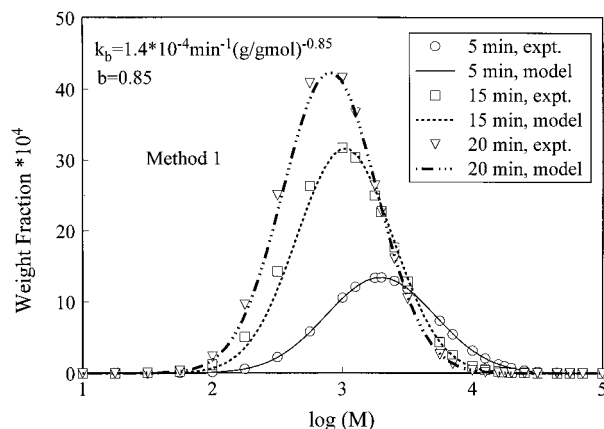


Figure 3 Log-normal molecular weight distribution curve for experimental (method 1) and predicted parameters.

A single value of b predicts standard deviations of the distribution that change monotonically with time. Equations (9)–(11) were solved numerically for several values of b (0, 0.85, and 1.0) and various $k_b \cdot t$ values. The resulting trends in $\log(M_m)$ and σ are shown in Figure 5. The intersection point of all the plots is the 5-min experiment ($M_m = 4,920$ and σ of 0.96), taken as the starting point for kinetic analysis. The data was extrapolated to predict the zero run parameters (M_m and σ) for $b = 0.0, 0.85,$ and 1.0 for various $k_b \cdot t$ s assuming that the degradation order remains the same. The values for M_m and σ obtained experimentally were (open circle) 13,040 and 0.93, respectively. The extrapolation for $b = 0.85$ (solid cross) gives a M_m 30,040 and a

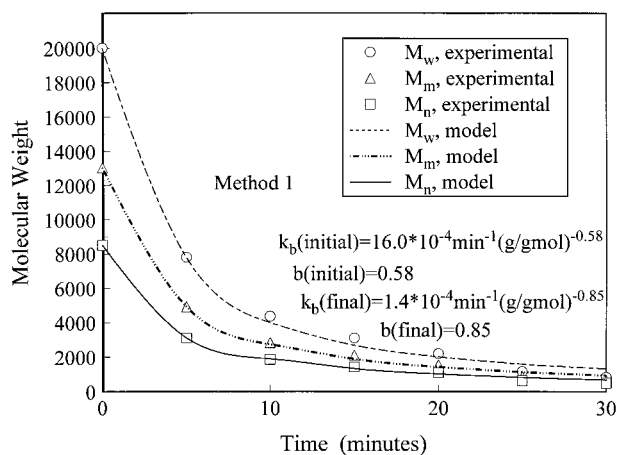


Figure 4 Molecular weight averages as function of reaction time: Comparison of experimental (method 1) and predicted data.

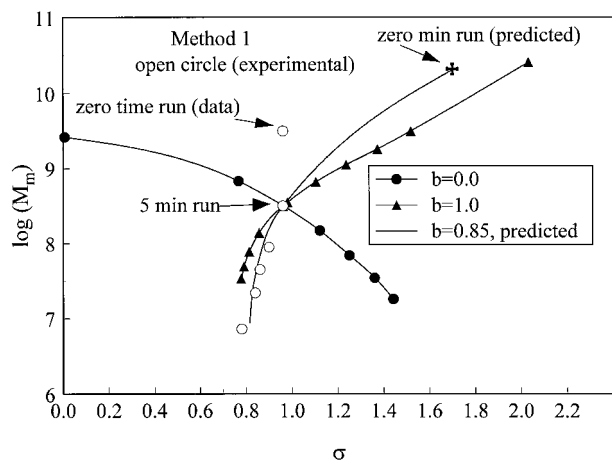


Figure 5 Comparison of the trends in log-normal distribution parameters, $\log(M_m)$ and σ , for constant value of the exponent b in the rate equation.

corresponding σ of 1.7 within 10% error; the model parameters do not extrapolate well to the zero time data. Furthermore, after 30 min of degradation time, the experimental data appear to shift away from the $b = 0.85$ curve as more gaseous products are formed. This suggests that a single set of kinetic parameters could not fit the entire distribution.

Hence, a two-stage breakdown of polyethylene in two different MW ranges is proposed, which is supported by literature studies.²² For method 1 runs, two sets of kinetic parameters were needed to model the kinetic product distributions. The first stage degradation for method 1 ($M_m > 5,000$) has a b value of 0.58 and a corresponding $k_b = 16.0 \cdot 10^{-4} \text{ min}^{-1} (\text{g/gmol})^{-0.58}$. When values of M_m and σ for the five time run are extrapolated to the zero time run, we get a $M_n = 98,000$ and $M_w = 160,000$, which is close to the actual values of 97,600 and 186,000 calculated of the virgin polymer (Fig. 6). As M_m approaches a value < 5000 ($\sigma \sim 0.96$), the degradation rate changes. The second set of kinetic parameters for method 1 were $k_b = 1.4 \cdot 10^{-4} \text{ min}^{-1} (\text{g/gmol})^{-0.85}$ and $b = 0.85$.

Method 2 had long heat-up times, and the molecular weights at zero time were $M_n = 2,820$ ($M_w = 13,150$), which would fall in or near the second stage rates. Only 1 set of parameters (second stage) is needed to describe this data as it has only 1 degradation rate. Furthermore, the parameters are consistent with those found for method 1 [$k_b = 1.4 \cdot 10^{-4} \text{ min}^{-1} (\text{g/gmol})^{-0.85}$ and $b = 0.85$].

Changes in the crystallinity of the product are consistent with a preferential degradation of long chains. The starting virgin polymer was found to have an amorphous portion of $\sim 50\%$ by solid state nuclear magnetic resonance (NMR)²³ [differential scanning calorimetry (DSC) analysis: 48%]. At 5 min (method 2), the amorphous portion of the polymer is less than half the original value, showing that its rate of degradation is faster than the crystalline portion.

For the 25- and 30-min runs, the model predicted a slightly higher value of the molecular weight averages than measured by GPC. Degradation rates for light model compounds (MW < 300) show that gas phase reactions can have significant impact.¹⁸ As time increases, the proportion of the gas phase increases as more volatiles are formed. Using $b = 0.85$ and molecular weight of 226 (hexadecane), the rate constant was calculated to be $2.4 \cdot 10^{-4} \text{ s}^{-1}$. Wu et al.¹⁸ obtained a first-order rate constant of $3.0 \cdot 10^{-4} \text{ s}^{-1}$. This discrepancy in our data can be attributed the lack of consideration of retrograde condensation products in our kinetic analysis. Also, we have not included the simdistillation results in our estimation of rate constant. For a small molecule like C_{16} , this could cause a large error.

Simdistillation is used in the oil industry to determine the distributions of C_7 through C_{40} compounds. Figure 7 shows that both the experimental methods (solid symbol, method 1; open symbol, method 2) gave similar levels of low-molecular-weight liquids as a function of reaction time. The model can be used to simulate the weight fractions of a given molecular weight

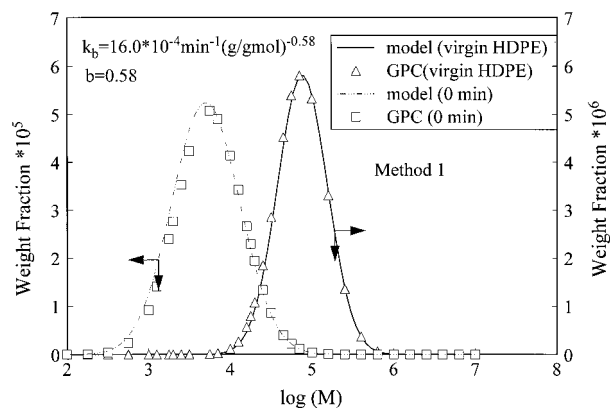


Figure 6 Molecular weight averages as a function of reaction time: Comparison of experimental (method 1) and predicted data for the virgin polymer from zero-time run.

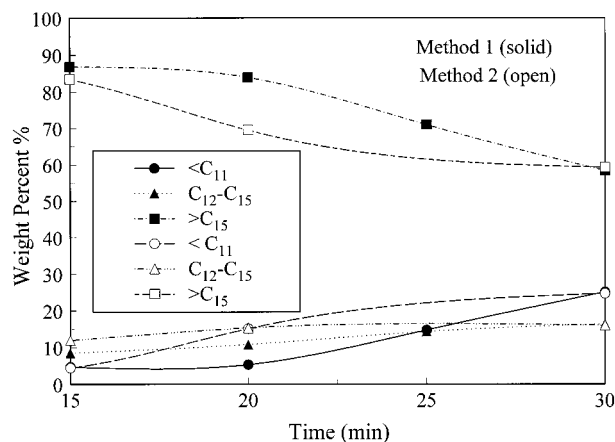


Figure 7 Simdistillation results of the product distributions of the kinetic runs as a function of reaction time (methods 1 and 2).

range of the polymer for a given time of liquefaction (Fig. 8). This prediction of the product distribution can be used to design the liquefaction process. The MW range 2000–5000 peaks at 10 min and gradually drops down as the reaction time increases. On the other hand, the MW range 1000–1500 is maximum at 25 min and slightly curves down beyond this time (up to 30 min).

Model Verification for Other Literature Data

Our method can be used to evaluate other reported data on polyethylene degradation. For example, we have used the data of Uddin et al.³ on the thermal analysis of HDPE to estimate their $k_b \cdot t$ and b . Their initial and final distributions had a M_m and σ corresponding to 534,700 and 1.26 and 26,000 and 0.83, respectively. We ob-

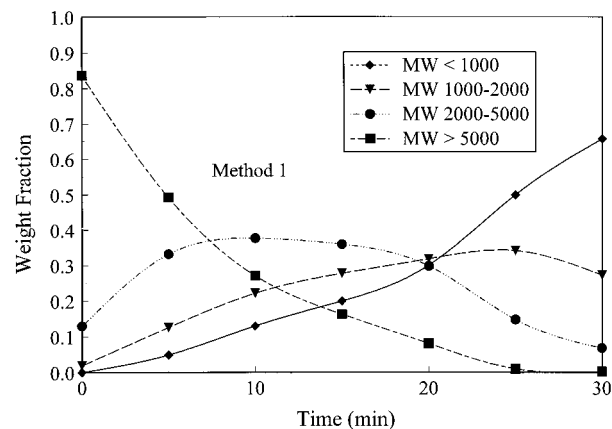


Figure 8 Simulation profiles of different MW ranges of samples of product obtained from model prediction as a function of reaction time.

tained b of about 0.8 and $k_b \cdot t = 7.5 \cdot 10^{-5} \text{ min}^{-1} (\text{g/gmol})^{-0.8}$. Uddin et al. had 2-h degradation times, and yet our estimate of their b value is similar to that found in this work. This suggests that our technique be useful in interpreting degradation of similar polymers.

TGA Curves

TGA analyses were used to estimate the temperature at the onset of degradation (devolatilization) and hence estimate the products in the sample from alkane boiling points. The onset temperature of devolatilization decreased as the time of reaction increased, indicating that the residual mixture has shorter molecules, thereby initiating faster chain breakdown. Table IV shows the onset temperature of devolatilization with time of liq-

Table III Molecular Weight Distribution Parameters: Comparison of Predicted and Experimental (Method 2 Experiments) Results

Time (min)	Experimental				Model			
	M_n	M_w	σ	M_m	M_n	M_w	σ	M_m
Virgin	97,600	185,700	0.802	134,600	98,000	160,000	0.7	125,200
0	2,820	13,150	1.24	6,080	2,820	13,150	1.24	6,080
5	1,700	4,460	0.98	2,750	1,750	4,270	0.95	2,730
10	1,190	2,630	0.95	1,770	1,230	2,660	0.88	1,810
15	950	2,000	0.86	1,380	940	1,940	0.85	1,350
20	720	1,440	0.83	1,020	750	1,510	0.83	1,070
25	660	1,260	0.80	920	630	1,240	0.83	880
30	590	880	0.63	720	540	1,050	0.82	750

$$k = 1.5 \cdot 10^{-4} \text{ min}^{-1} (\text{g/gmol})^{-0.85}, b = 0.85.$$

Table IV Prediction of Oligomeric Species from TGA and Boiling Point Curve of Alkanes

Time of Reaction (min)	Onset Temperature of Devolatilization (°C)	Species (Method 2)	Onset Temperature of Devolatilization (°C)	Species (Method 1)
Virgin HDPE	453	$>C_{33}H_{68}$	453	$>C_{33}H_{68}$
0	319	$>C_{18}H_{38}$	323	$>C_{19}H_{40}$
5	289	$>C_{16}H_{34}$	314	$>C_{18}H_{38}$
10	260	$>C_{14}H_{30}$	295	$>C_{17}H_{36}$
15	241	$>C_{13}H_{28}$	265	$>C_{15}H_{32}$
20	184	$>C_{10}H_{22}$	249	$>C_{14}H_{30}$

uefaction and the corresponding saturated hydrocarbon having a normal boiling point similar to the onset temperature of devolatilization. The majority residual species present in the TGA pan have a molecular weight greater than that of the alkane listed. These data are consistent with the molecular weight data in Table III. As an example, the thermogram (Fig. 9) for the 20-min run for method 1 showed that 60% weight fraction was left in the sample pan at 300°C. The simdistillation of the waxes indicated that 77% of sample had a boiling point greater than 300°C. This is reasonable agreement since TGA data also includes continuous degradation.

Part 3: Mixed Plastic Waste Liquefaction

The random chain scission model was used to analyze the DSD plastic degradation. The M_n and M_w of the starting polymer mixture were 175,000 and 407,000. The results are given in Table V.

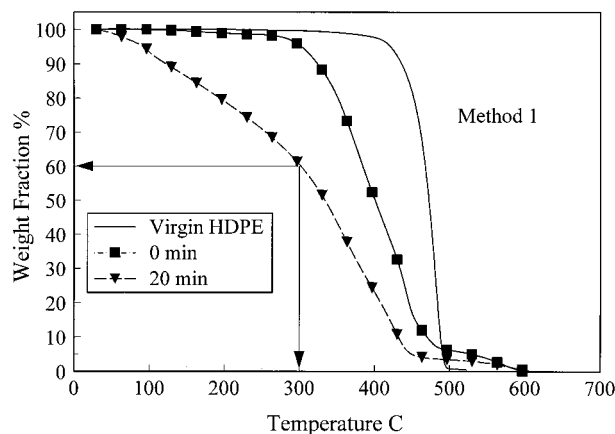


Figure 9 HDPE liquefaction thermograms for 0- and 20-min runs (weight loss as a function of temperature).

From these results, an estimate of the rate constants of degradation at different temperatures studied, and, hence, the activation energy for the degradation of the plastic mixture were obtained. A b value of 0.83 was obtained; this represents the cumulative effect of PE, PS, and other components in the waste plastic. Polyethylene degradation in the presence of catalysts is known to produce lighter product fractions. This liquefaction was, however, conducted thermally without any added catalyst. Minor amounts of polymerization catalysts could affect the product molecular weight distribution; however, these were also present in the HDPE sample, on which we did liquefaction earlier. Thus, b is not significantly altered in the presence of other polymers. However, the pseudo-first-order rate constants k_b obtained are an order of magnitude higher than that for HDPE. One reason for this could be the method of experimentation. The analysis was carried out considering the zero-time run as the starting polymer itself since the time of liquefaction is large compared to the heat up time. Hence, the rate constant depicted here could be the combination of the faster and slower rate constants of both the stages of degradation. Calibration of the GPC was done based on polyethylene since it formed the major component of the plastic. However, the calibration cannot be valid because the viscosity of the polymer mixture is not known. The errors obtained in computation (about 15%) can be attributed to that. Since most of the sample is polyethylene, the model fits reasonably well.

A mean activation energy of 63.0 kcal/mol was obtained for random chain scission kinetics. The frequency factor was $1.9 \times 10^{15} \text{ min}^{-1}$. Literature studies have assigned values between 63 and 71

Table V Mixed Plastic (DSD) Results: Values of k_b Obtained by Data Fitting to Model ($b = 0.83$)

$k_b \cdot 10^3$ [$\text{min}^{-1} (\text{gm/gmol})^{-0.83}$]	M_n	M_w	M_n (exp)	M_w (exp)	Exp T (°C)
1.2	4240	7660	4070	7880	415
1.7	2860	5300	2770	5360	420
2.3	2230	3490	1990	3860	425
4.5	950	1660	880	1700	435

kcal/mol.¹⁵ Branching might be a factor due to which the range of activation energies have been given. The frequency factor was $1.9 \cdot 10^{15} \text{ min}^{-1}$. In the presence of catalyst, the activation energy dropped to 45.0 kcal/mol and the corresponding frequency factor was $5.3 \cdot 10^9 \text{ min}^{-1}$.

CONCLUSIONS

Production of liquid products from HDPE liquefaction has a maximum yield between 450 and 460°C. The oil product had higher fractions of light oils (two-fold increase) at higher temperature. Hydrogen at 450°C did not significantly alter the product distribution and did not affect the degradation rate parameters for polyethylene.

We developed a numerical method for solving the moments approach to random chain scission degradations. As was found for model compounds, the random chain scission rates varies with the molecular weight of the reacting species by a power law dependence. The model suggests that HDPE degrades via a two-stage process in which high-molecular-weight material is quickly degraded to a moderate molecular weight [$k_b = 16.0 \cdot 10^{-4} \text{ min}^{-1} (\text{g/gmol})^{-0.58}$, $b = 0.58$], followed by lower degradation rates for lower-molecular-weight material [$k_b = 1.4 \cdot 10^{-4} \text{ min}^{-1} (\text{g/gmol})^{-0.85}$, $b = 0.85$]. The method can be applied to optimize liquid fraction yield and can be applied to other waste plastic mixtures.

This research is supported by the US DOE, as part of the research program of the Consortium for Fossil Fuel Liquefaction Science. The authors acknowledge the help obtained from the correspondence with Prof. McCoy, UC Davis. Also, the authors thank Dr. Huffman's group for simdistillation analyses and DSD samples of and Dr. Pugmire, University of Utah, for the valuable advice and equipment use for solid state NMR studies.

NOMENCLATURE

b :	exponent of molecular weight in rate constant expression for chain scission
k_b :	pseudo-first-order rate constant for chain scission
$k(x)$:	rate constant expression for chain scission
M_m :	log-normal distribution median value
M_n :	number-average molecular weight for a given MWD
M_n^0 :	initial number-average molecular weight for the distribution
M_w :	weight-average molecular weight for a given MWD
M_w^0 :	initial weight-average molecular weight for the distribution
M_z :	z average molecular weight for a given MWD
M_{z+1} :	$z + 1$ average molecular weight for a given MWD
p^i :	i th moment for the given MWD
$p(x)$:	MWD of sample at any given time t
$p_0(x)$:	initial MWD of sample
$p_n(x)$:	mole fraction MWD
$p_w(x)$:	weight fraction MWD
σ :	standard deviation for the log-normal MWD
$\Omega(x, x')$:	stoichiometric kernel satisfying the normalization and symmetry conditions
t :	time
x :	molecular weight of the species

APPENDIX

We have modeled liquefaction kinetics based on the degradation model applied for poly(styrene) allyl alcohol, based on random chain scission. For

$b = 0$, the analytical solution was provided by Wang et al.⁴ These, when coupled with our definitions of M_n and M_w give

$$M_n = M_n^0 \cdot \exp(-k_b \cdot t)$$

$$M_w = M_w^0 \cdot \exp(-\frac{1}{3} k_b \cdot t)$$

For $b = 1$, we can manipulate equations (9)–(11). Since p^1 is constant with time (mass conservation), we can divide the first and last equations by p^1 . Hence, we get

$$\frac{d(1/M_n)}{dt} = k_b$$

$$\frac{1}{M_n} = \frac{1}{M_n^0} + k_b \cdot t$$

To obtain M_w ,

$$\frac{dM_w}{dt} = \left(-\frac{1}{3} k_b \cdot \frac{p^3}{p^1} \right)$$

$$\frac{dM_w}{dt} = -\frac{1}{3} k_b \cdot \frac{p^3}{p^2} \cdot \frac{p^2}{p^1}$$

$$\frac{dM_w}{dt} = -\frac{1}{3} k_b \cdot M_z \cdot M_w$$

$$\frac{dM_w}{dt} = -\frac{1}{3} k_b \cdot \frac{M_w^3}{M_n}$$

$$\frac{dM_w}{dt} = -\frac{1}{3} k_b \cdot M_w^3 \cdot \left(\frac{1}{M_n^0} + k_b \cdot t \right)$$

$$\frac{1}{M_w^2} = \frac{1}{(M_w^0)^2} + \frac{2}{3} \frac{k_b \cdot t}{M_n^0} + \frac{k_b^2 \cdot t^2}{3}$$

Here, M_z is the z -average molecular weight distribution given by p^3/p^2 , as follows:

$$M_z = M_m \exp\left(\frac{3\sigma^2}{2}\right) = \frac{M_w^2}{M_n}$$

This can be extended to subsequent values of b . For example,

$$M_{z+1} = M_m \exp\left(\frac{5\sigma^2}{2}\right) = \frac{M_z^2}{M_w}$$

Hence, integer values of b can be solved by using the relationship of log-normal distribution functions. When these equations were solved by a 4th-order Runge–Kutta method, we got about 3% error for the $b = 1$ and $b = 0$ model. This is illustrated in Figure 2. For $b = 2$, we get, using (9), (10), and (11),

$$\frac{d(1/M_n)}{dt} = k_b \cdot M_w$$

$$\frac{dM_w}{dt} = \left(-\frac{1}{3} k_b \cdot \frac{p^4}{p^1} \right)$$

$$\frac{dM_w}{dt} = -\frac{1}{3} k_b \cdot \frac{p^4}{p^3} \cdot \frac{p^3}{p^2} \cdot \frac{p^2}{p^1}$$

$$\frac{dM_w}{dt} = -\frac{1}{3} k_b \cdot M_{z+1} \cdot M_z \cdot M_w$$

Using relation for M_z and M_{z+1} , we get

$$\frac{dM_w}{dt} = -\frac{1}{3} k_b \cdot \frac{M_w^6}{M_n^3}$$

From the equations for M_w and M_n as a function of t , we get

$$\frac{dM_n}{M_n^5} = 3 \frac{dM_w}{M_w^5}$$

Integrating within limits M_n^0 to M_n and M_w^0 to M_w ,

$$\frac{1}{M_w^4} = \frac{1}{3} \left(\frac{1}{M_n^4} - \frac{1}{(M_n^0)^4} \right) + \frac{1}{(M_w^0)^4}$$

Thus, we get a single equation in M_n as

$$\frac{dM_n}{dt} = -k_b \cdot M_n^2 \cdot \left(\frac{1}{3} \left(\frac{1}{M_n^4} - \frac{1}{(M_n^0)^4} \right) + \frac{1}{(M_w^0)^4} \right)^{(-1/4)}$$

The above equation can be solved numerically to get a relation of M_n with t , which can be substituted to get M_w (Fig. 2). This treatment of data can be used for all integral values of $b \geq 2$.

REFERENCES

1. M. V. S. Murty, P. Rangarajan, E. A. Grulke, and D. Bhattacharyya, *Fuel Process. Technol.*, **49**, 75 (1996).
2. S. H. Ng, H. Seoud, and M. Stanciulescu, *Energy Fuels*, **9**, 735 (1995).
3. M. A. Uddin, K. Koizumi, K. Murata, Y. Sakata, *Polym. Degrad. Stab.*, **56**, 37 (1997).
4. M. Wang, J. M. Smith, and B. J. McCoy, *AIChE J.*, **41**, 1521 (1995).
5. G. Madras, J. M. Smith, and B. J. McCoy, *Ind. Eng. Chem. Res.*, **35**, 1795 (1996).
6. P. L. Beltrame, P. Carniti, G. Audisio, and F. Bertini, *Polym. Degrad. Stab.*, **26**, 209 (1989).
7. M. Weiland, A. Daro, and C. David, *Polym. Deg. Stab.*, **48**, 275 (1995).
8. F. E. Okieimen and J. E. Ebhoaye, *J. Appl. Polym. Sci.*, **48**, 1853 (1993).
9. S. Al-Malaika, S. Chohan, M. Coker, and G. Scott, *Pure Appl. Chem.*, **A32**, 709 (1995).
10. I. C. McNeill and M. Bounekhel, *Polym. Deg. Stab.*, **34**, 187 (1991).
11. B. J. McCoy and M. Wang, *Chem. Eng. Sci.*, **49**, 3773 (1994).
12. M. Wang, C. Zhang, J. M. Smith, and B. J. McCoy, *Energy Fuels*, **8**, 890 (1994).
13. M. Wang, J. M. Smith, and B. J. McCoy, *Energy Fuels*, **7**, 78 (1993).
14. Sir G. Allen, Ed., *Encyclopedia of Polymer Science*, Vol. 6, *Thermal Degradation*, 1st ed., 1989, pp. 467–468.
15. H. F. Mark, M. G. Garyland, and N. M. Bilkes, Eds., *Encyclopedia of Polymer Science and Technology, Depolymerization*, 1988, pp. 719–745.
16. H. H. Voge and G. M. Good, *J. Am. Chem. Soc.*, **71**, 593 (1949).
17. R. Aris and G. R. Gavalas, *Phil. Trans. R. Soc. London*, **A260**, 351 (1966).
18. G. Wu, Y. Katsumura, C. Matsuura, and K. Ishigure, *Ind. Eng. Chem. Res.*, **35**, 4747 (1996).
19. A. Kossiakoff and F. O. Rice, *J. Am. Chem. Soc.*, **65**, 590 (1943).
20. L. L. Anderson, W. Ding, and J. Liang, *Proceedings of the Consortium of Fossil Fuel Liquefaction Sciences Conference*, 1996, pp. 101–111.
21. Z. Feng, J. Zhao, J. Rockwell, D. Bailey, and G. P. Huffman, *Fuel Proc. Technol.*, **49**, 17 (1996).
22. T. Kuroki, T. Sawaguchi, S. Niiikuni, and T. J. Ikemura, *J. Polym. Sci.*, **21**, 703 (1983).
23. *Proceedings of the Consortium for Fossil Fuel Liquefaction Sciences Conference*, 1997.